

ORIGINAL RESEARCH

OPEN ACCESS
Full open access to this and
thousands of other papers at
<http://www.la-press.com>.

Homology Modeling and Molecular Dynamics Simulation Studies of a Marine Alkaline Protease

Xiaofeng Ji, Wei Wang, Yuan Zheng, Jianhua Hao and Mi Sun

Yellow Sea Fisheries Research Institute, Chinese Academy of Fishery Sciences, Qingdao, Shandong, China.
Corresponding author email: sunmi@ysfri.ac.cn

Abstract: A cold-adapted marine alkaline protease (MP, accession no. ACY25898) was produced by a marine bacterium strain, which was isolated from Yellow Sea sediment in China. Many previous researches showed that this protease had potential application as a detergent additive. It was therefore crucial to determine the tertiary structure of MP. In this study, a homology model of MP was constructed using the multiple templates alignment method. The tools PROCHECK, ERRAT, and Verify_3D were used to check the effectiveness of the model. The result showed that 94% of residues were found in the most favored allowed regions, 6% were in the additional allowed region, and 96.50% of the residues had average 3D-1D scores of no less than 0.2. Meanwhile, the overall quality factor (ERRAT) of our model was 80.657. In this study, we also focused on elucidating the molecular mechanism of the two “flap” motions. Based on the optimized model, molecular-dynamics simulations in explicit solvent environments were carried out by using the AMBER11 package, for the entire protein, in order to characterize the dynamical behavior of the two flaps. Our results showed an open motion of the two flaps in the water solvent. This research may facilitate inhibitor virtual screening for MP and may also lay the foundation knowledge of mechanism of the inhibitors.

Keywords: marine alkaline protease, homology modeling, molecular dynamic simulation, zinc-metalprotease, explicit water

Bioinformatics and Biology Insights 2012:6 255–263

doi: [10.4137/BBI.S10663](https://doi.org/10.4137/BBI.S10663)

This article is available from <http://www.la-press.com>.

© the author(s), publisher and licensee Libertas Academica Ltd.

This is an open access article. Unrestricted non-commercial use is permitted provided the original work is properly cited.



Introduction

Proteases execute a large variety of functions and have important biotechnological applications.¹ They represent one of the largest groups of industrial enzymes and are used in the detergent, leather, food, and pharmaceutical industries, as well as in bioremediation processes.² They are currently classified into six broad groups: serine proteases, threonine proteases, cysteine proteases, aspartate proteases, metalloproteases, and glutamic acid proteases. The metzincin family of metalloproteinases is so named for the zinc binding motif HEXXHXXGXXH and a conserved methionine, which is located on a turn near the base of the metal binding pocket.³ Among this family, some enzymes from a host of permanently cold habitats have been paid more and more attention. In recent years, there has been growing interest in cold-adapted enzymes as models in basic studies. Studies have attempted to investigate the thermal stability of these proteins and to understand the relationship between their stability and catalytic efficiency and their potential as candidates for industrial and biotechnological applications.^{4,5} The cold-adapted marine alkaline protease (MP, accession no. ACY25898) is one of these enzymes.

The MP molecule is a metallo endoprotease, which is made up of 480 amino acid residues. It is about 49 kD with an isoelectric point of about 4.5. It exhibits maximum activity at 30 °C, stability at pH values between 8 and 11, and insensitivity to phenylmethanesulfonyl fluoride. Sequence alignment and our previous study revealed that this protein belonged to the serralyisin-type metalloproteases,⁶ which in turn belong to the metzincin metalloprotease superfamily.⁷ From the obvious study on the sequence of MP, we found the sequence segment HEIGHTLGLSH in the protein. This segment was equivalent to the zinc binding motif HEXXHXXGXXH. In addition, we also found that there are four continuous calcium-binding domains which increased the thermal stability of MP. This protein is homologous to *Pseudomonas aeruginosa* protease (AP, PDBid: 1H71_A), psychrophilic alkaline protease (PAP, PDBid: 1JIW_P), and *Serratia marcescens* protease (SMP, PDBid: 1SAT_A), with strong similarity of more than 60%. Compared with mesophilic enzymes, cold adapted enzymes are usually more flexible. They usually have looser surface loops and weaker hydrogen bonding.

Similar to PAP, MP is a cold adapted protease, but they have different living environments, namely temperature. Structural studies are important to elucidate the structure-environment adaptation of these proteases. In order to get some explanations about the differences in their biochemical properties, modeling the tertiary structure of MP became important. The interaction between enzyme and its ligands is often accompanied by changes in the conformation of the residues within the active site region. In AP, PAP, and SMP, there is a particular structural feature that two of the four loops surrounding the active-site region can flap. The two flaps corresponding to residues 126–129 and 182–189 in PAP play a role in restricting the access to the substrate binding cleft, and thus in controlling the substrate specificity.^{8,9} In MP, are there two flaps, just like PAP? To solve this problem, a twenty nanosecond-duration constrained molecular dynamics (MD) calculation in water was undertaken in an attempt to predict and understand the conformational changes of the two flaps. Molecular dynamics (MD) simulation was undertaken by using the AMBER11 software package.¹⁰

In the present study, we focused on the investigation of MP homology modeling and explicit molecular dynamic simulation of two flaps. Our results show that the proper combination of homology modeling and MD simulation is powerful in predicting protein structure and obtaining a detailed description of the active site at the atomic level. The modeled structure will give us a better understanding of the relationship between protein structure and its function. Meanwhile, the modeled structure of MP will be of importance in the screening and designing of its inhibitor. This structure may also facilitate its industrial applications.

Materials and Methods

Homology modeling

Homology modeling and molecular dynamic (MD) techniques were utilized to construct the three-dimensional structure of MP. The target sequence of MP (accession no. ACY25898) was downloaded from the National Center for Biotechnology Information (NCBI) protein database. Meanwhile, a sequence similarity search for this protease against sequences from the Protein Data Bank (PDB) database was performed on the BLAST online server



(<http://blast.ncbi.nlm.nih.gov>).¹¹ We then found from the PDB that there were sixteen structures identified as homologous. They shared no less than 50% sequence identity with the query sequence. It was noteworthy that after excluding the redundant results, there were only three proteases (AP, PAP and SMP) left. Hence, they were selected as the template. The automated sequence alignment and analysis of the template and target was carried out using Esript2.2.¹² The Risler matrix was used to calculate the similarity score, with the similarity global score set to 0.7. The tertiary structure of MP was built using MODELLER¹³ (version 9.9), which was used for homology modeling of protein three-dimensional structures. The predicted structures were saved in the PDB format and sorted according to scores calculated from discrete optimized protein energy (DOPE)^{14,15} scoring and GA341.¹⁶ To assess the quality of the optimized models PROCHECK,¹⁷ ERRAT,¹⁸ and Verify_3D¹⁹ analyses were also undertaken.

Molecular dynamics simulations

In this study, two separate sets of MD simulations were undertaken by using the Amber11 package. One was the model refinement, which was used to reduce steric clashes among residues. The other was focused on modeling the motion of the corresponding flaps.

The constructed model had to be refined because the changed side-chains could affect the backbone, which would have an effect on the predicted conformations. The constructed model was subjected to an energy minimization process by using the conjugate gradient method for about 10000 iterations and 2 ns isothermal, constant volume MD simulation, with AMBER FF03, all hydrogen amino acid parameters, and the TIP3P water box.

Using the refined model as the starting structure, another MD simulation was focused on modeling the conformation changes of two flaps. All bonds involving hydrogen atoms were constrained with the SHAKE²⁰ algorithm. Eleven Ca²⁺ ions were added to obtain charge neutrality. The systems were then solvated using the simple explicit water model. For explicit water simulation, a cubic box was set up and the molecules were positioned at the center of the box by defining a 10 Å distance between the protein and the box edge. The systems were minimized with the SANDER program using 2500 steps of the steepest

descent algorithm, followed by 5000 steps of the conjugated gradient algorithm. The PMEMD program was used for molecular dynamics simulations.

Firstly, the restraining forces were applied to all atoms of the protein with 500 kcal/mol for 100 ps. Then, all constraints were removed and the whole system was minimized for 100 ps. Secondly, the whole system was heated from 0 K to 300 K in water over 500 ps, with constraints applied to all backbone atoms, followed by 20 ns of simulation where the proteins were free to move. The simulations were carried out for a total of 20 ns at constant temperature (303 K) and pressure (1 bar) conditions and the integration step was 2 fs. To avoid artifacts, five MD simulations were run twice, with different starting atomic velocities from the Maxwellian distribution. The resulting trajectories were analyzed using the Ptraj module of the AMBER 11 package. The RMSD was calculated for the protein backbone atoms using least-squares fitting. Distances between given residues were calculated with the position for Ca atoms.

Other calculations

Ligplo²¹ is a program used to plot schematic diagrams of protein-ligand interactions for a given ligand in a PDB file. In this study, this software was used to create a 2D diagram of hydrophobic and hydrogen bonding interactions for the Zn²⁺ ion and the coordinate residues.

Results and Discussion

Sequence alignment

An optimal sequence alignment is essential to the success of homology modeling. We performed the sequence alignment on the clustalw²² server at the EBI²³ using the default parameters. A consensus sequence was generated using criteria from MULTALIN²⁴ and the result was shown in the bottom of Figure 1. The relative accessibility of each residue was extracted from DSSP²⁵ and PHD²⁶ files. The alignment results showed that the MP displayed 91% sequence identity with PAP and 63% with AP. Meanwhile, the flap loops of MP and PAP were strictly conserved and the conserved flaps were 140–147 and 237–243 in corresponding positions of MP.

Model construction and refinement

Because of the importance of metallo-endoproteases in many diseases (eg, cancer and arthritis) and to in

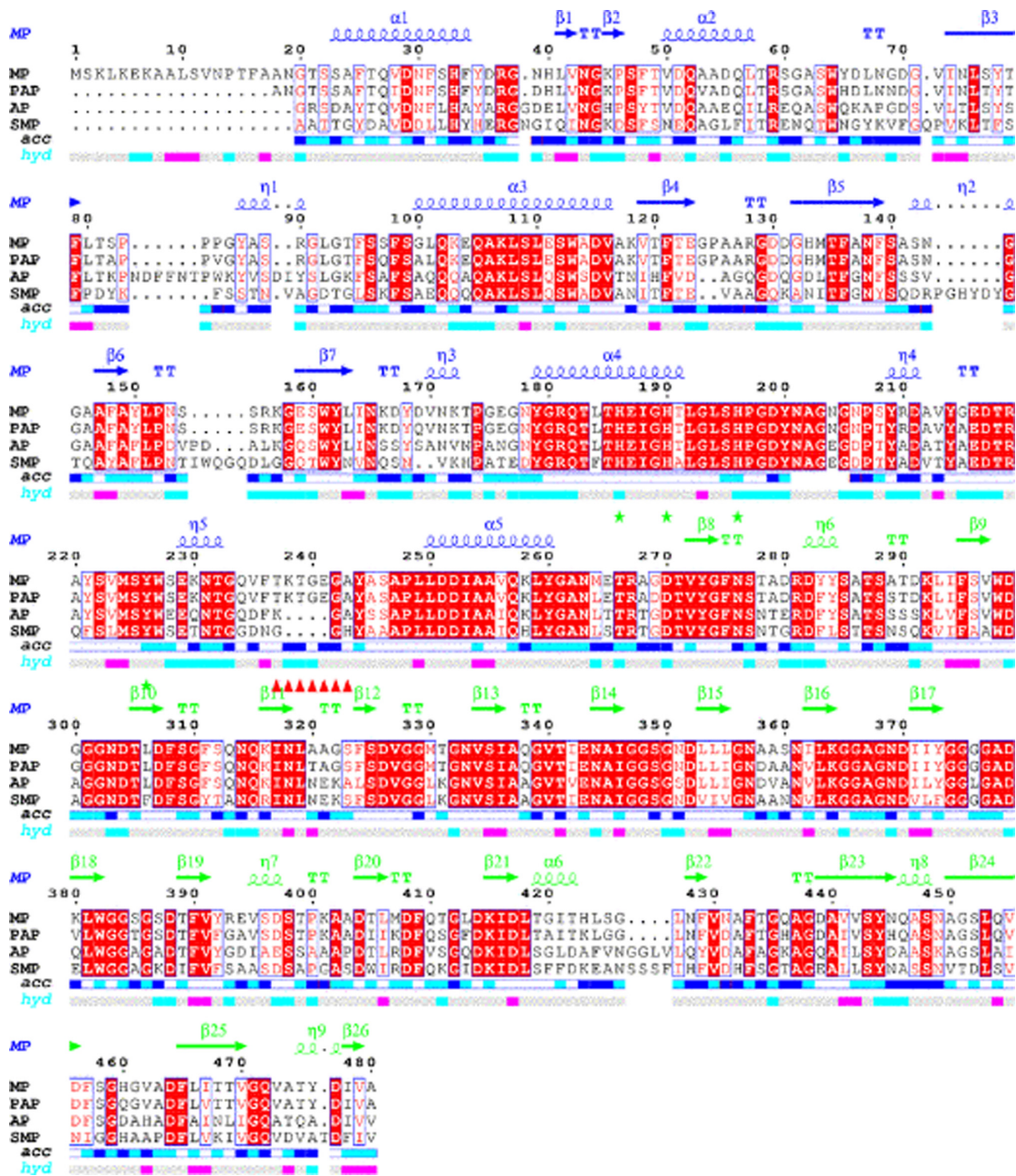


Figure 1. Sequence alignment for MP, PAP, AP and SMP.

Notes: Secondary structure elements for MP are indicated in blue for the catalytic domain and in green for the C-terminal domain. The relative accessibility of each residue is rendered as blue-colored boxes from dark blue (accessible) to white (buried residues). The hydropathic character of the sequence calculated according to the algorithm of Kyte and Doolittle with a window of 3 is also shown, with the color varying from pink (hydrophobic) through grey (intermediate) to cyan (hydrophilic). HIS186, HIS190, HIS196 and Tyr226 of the active site are marked as green star. Furthermore, the loop (K237-A243) is marked as red triangles. The presentation of the sequence alignment was made using the online service of ESPript2.2.

order to get a better understanding of the experimental findings, especially to predict substrate specificity of MP, it was critical to know the three-dimensional structure of MP. In this study, homology modeling technique was used to construct models of MP based on the strong similarity among the structures of marine alkaline protease (MP), *P. aeruginosa*

(AP), psychrophilic alkaline protease (PAP) and *S. marcescens* (SMP).

The homology modeling approach was used to construct the structure of MP using MODELLER9v9. In Table 1, the five resulting three-dimensional models of MP are listed. They were sorted according to DOPE and GA341 score. From the table, we can see that

Table 1. The top 5 results of modeled structures.

File name	molpdf	DOPE score	GA341 score
B1.pdb	2234.95557	-48413.07812	1.00000
B2.pdb	2314.27441	-48484.16406	1.00000
B3.pdb	2323.42920	-48720.34375	1.00000
B4.pdb	2339.14673	-48777.64453	1.00000
B5.pdb	2186.03101	-48820.30469	1.00000

the GA341 score all equal 1.00000 and their DOPE scores are all lower than -48000. By comprehensive analysis of these three scores, the B1.pdb was selected as the initial model. PROCHECK was used to evaluate the Stereochemical properties of the model. A Ramchandran plot was built and it showed that 92.9% of residues were in the most favored regions and 7.1% were in the additional allowed regions. After the MD refinement, the check process was also undertaken. The Ramchandran plot of our model showed that 94% of residues were found in the most favored allowed regions and 6% were in the additional allowed region. Verify-3D graphs showed that 96.50% of the residues had average 3D-1D scores of no less than 0.2. Thus, side chain environments are acceptable. Meanwhile, the overall quality factor (ERRAT) of our model was 80.657. Thus the model was acceptable and was chosen for subsequent molecular dynamical simulation.

The refined model is shown in Figure 2, as drawn by the Pymol²⁷ program. In this model, the MP protein had two domains and might have one Zn²⁺ in its active site. Its tertiary structure was comparable to those of the available homologues PAP with the N-terminal domain comprising residues 1-264 and the C-terminal domain comprising residues 265-480.

Catalytic domain and active site

From the above analysis we knew that MP was one of the Metzincins which had an essential Zn²⁺ for the catalytic activity. A feature that characterized this sub-family was the sequence motif HEXXHXXGXXHZ, wherein the histidine residues were ligands to the Zn²⁺ and Z was characteristic in the different subfamilies. This conserved segment corresponded to H186-P197 in MP. Moreover, a conserved methionine residue that was likewise characteristic of the metzincin superfamily was also present in MP (Met224). From the LigPlus result (Fig. 3), we could easily find that Zn²⁺ was bound to the side-chains of HIS186, HIS190, HIS196, TYR


Figure 2. General overview of the structure of MP.

Notes: The whole figure was generated by Pymol and shown in rainbow cartoon. The Zn²⁺ in the N-terminal domain is indicated as a magenta sphere.

226 and a water molecule. Meanwhile, the water molecule was also bound to the side-chain of Glu187 and TYR226, which was thought to be important in activating the water molecule during catalysis.²⁸ The hydroxyl group of this tyrosine served as the fifth ligand for the Zn²⁺. However, upon substrate binding, the tyrosine hydrogen bonded to the main chain of the bound peptide. Just as shown in Figure 4, the distance of the residues His 169, 173, 179, and Tyr209 to the zinc ion at the active site in PAP (1H71_A) are 2.29, 2.24, 2.26, and 2.96 respectively. However, in MP, the distance of residues His 186, 190, 196, and Tyr226 to the zinc ion are 2.20, 2.22, 2.0, 3 and 2.44 respectively (as shown in Fig. 3). In order to inspect whether the active zone is associated with histidine, we studied the relationship between the histidine residue and enzyme activity. Through the sequence analysis we know that there is no mercapto amino acid in this protein; therefore we used acetate bromine (BrAc) to modify this enzyme directly. We determined that the leaving enzyme activity after BrAc and the enzyme reacted 30 minutes in the NaAc-HAc buffer. The pH of the solution was 6.0 and the reaction temperature 30 °C. From the result, we

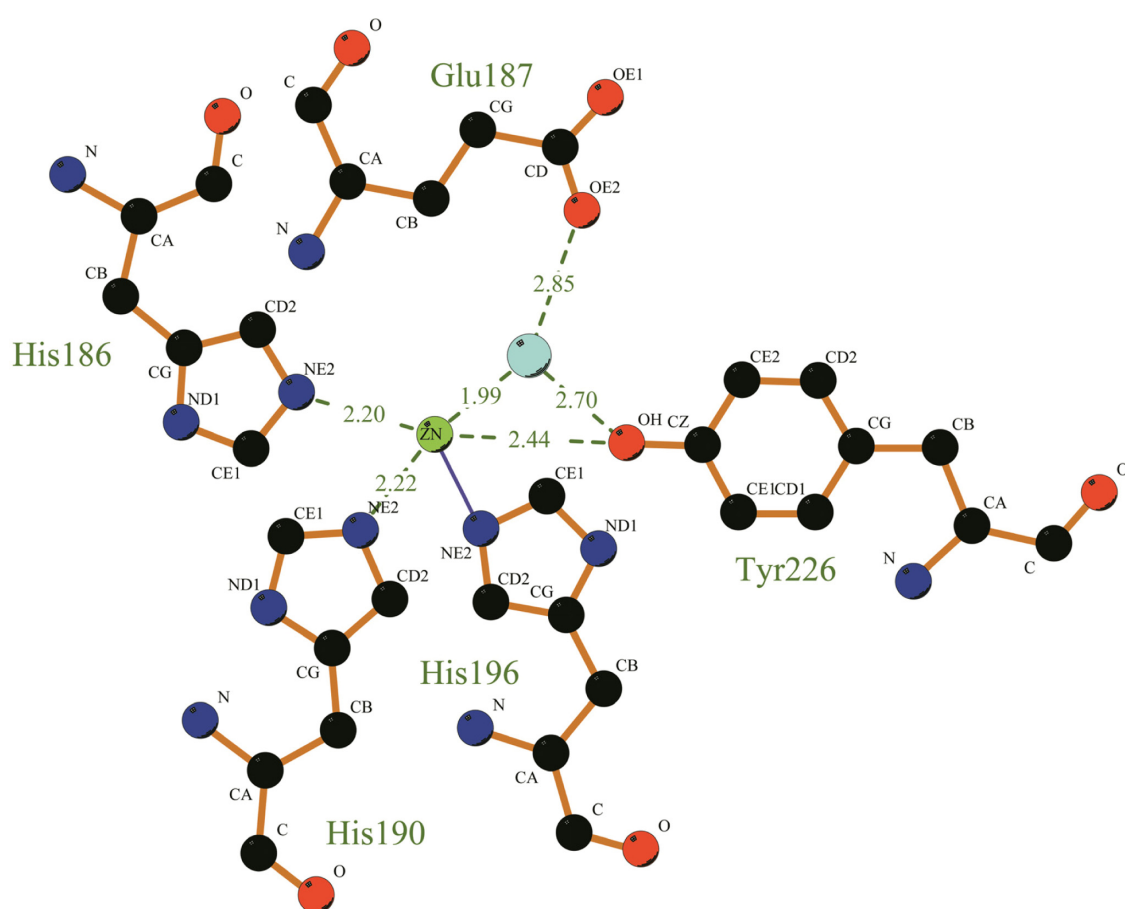


Figure 3. The molecular interaction of the active sites of MP.

Notes: Zn^{2+} and water are shown as spheres colored in light green and light blue respectively. Amino acid side chains are shown as sticks colored red for oxygen and blue for nitrogen. Hydrogen bonds are displayed using dashed lines while metal coordination bonds are indicated by green dashed lines. This figure was made using LigPlus.

found that, with the increase of BrAc's concentration, the relative activity decreased gradually. The binding site defined in DS client showed that this cavity could include 216 detector molecules and its volume was 27 \AA^3 (with the threshold set at 2.5 \AA). The position of the cavity center was $-14.866, 100.425, -5.154$, and the cavity radius was 5 \AA . In the active site, Zn^{2+} was coordinated with His 186, 190, 196, and Tyr226. Similar to PAP, they formed a coordinate in trigonal bipyramidal geometry to four or five ligands depending on the position of TYR226. Docking might occur within this range, which gave us something to inspect in a further study.

MD simulation

In order to investigate the motion of the two loops, the modeled structure was simulated by the explicit water MD and a 20 ns MD simulation was performed. The starting model was built from the homology modeling

of model1 described above. The MD simulation was run twice using different starting velocities to avoid artifacts. Because the movements of flaps in two MD simulations were the same, the analysis of only one MD simulation is described below.

As expected, a conformational change was observed during the MD simulation. The backbone RMSD of the conformation after 20 ns when compared to the initial structure was 3.025 \AA for the global structure (Fig. 4C). As far as flap1 (S140-A147) was concerned, there was a displacement of 2.6 \AA in the conformation after 20 ns and a displacement in the initial structure for Ca atoms of the G144 (Fig. 5A). This was different from the approximately 6 \AA in PAP. For flap2 (T237-A244), there was an evident conformation change. The distance between the Ca atoms of Thr239 was 16.3 \AA (Fig. 4B). This was in agreement with the generally accepted concept that cold adapted proteins were more flexible.

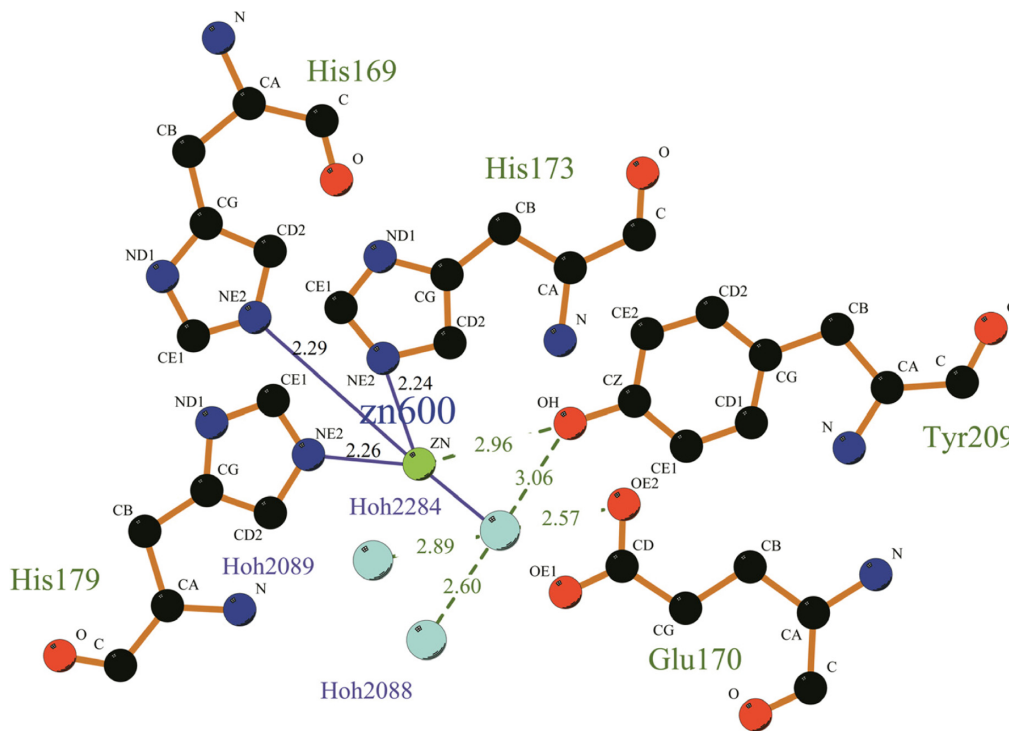


Figure 4. The molecular interaction of the active sites of PAP.

Notes: Zn^{2+} and water are shown as spheres colored in light green and light blue respectively. Amino acid side chains are shown as sticks colored red for oxygen and blue for nitrogen. Hydrogen bonds are displayed using dashed lines while metal coordination bonds are indicated by green dashed lines. This figure was made using LigPlus.

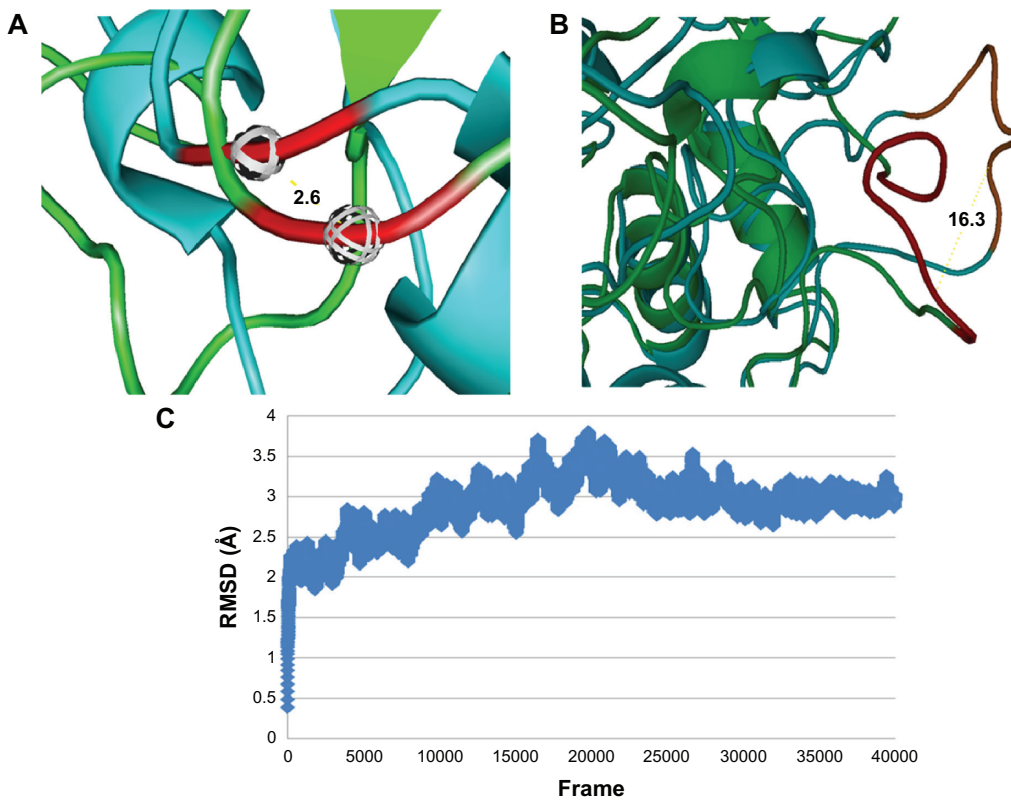


Figure 5. The trajectory of the MP was analyzed by calculating RMSD.

Note: 40000 frames are extracted from 20 ns trajectory.



Conclusion

We presented the optimized tertiary structure of MP by homology modeling method. The modeled structure of MP in this study allowed us to better understand the binding of Zn^{2+} . Because the substrate specificity of alkaline metalloproteases was controlled by the structural rearrangement of the two mobile loops, we performed large scale MD simulation that revealed the movement of two flaps. These results might further the understanding of the molecular design of inhibitors and facilitate the virtual screening of inhibitors for the cold-adapted marine alkaline protease MP.

Author Contributions

Conceived and designed the experiments: XJ, MS. Analysed the data: XJ, YZ, JH. Wrote the first draft of the manuscript: XJ. Contributed to the writing of the manuscript: XJ, WW. Agree with manuscript results and conclusions: XJ, WW, YZ, JH, MS. Jointly developed the structure and arguments for the paper: MS. Made critical revisions and approved in all version: XJ. All authors reviewed and approved of the in all manuscript.

Funding

This work is supported by the Specific International Cooperation and Exchanges in Science and Technology (2011DFB30250) and the National High Technology Research and Development Program ("863" Program) of China (2011AA090703).

Competing Interests

Author(s) disclose no potential conflicts of interest.

Disclosures and Ethics

As a requirement of publication author(s) have provided to the publisher signed confirmation of compliance with legal and ethical obligations including but not limited to the following: authorship and contributorship, conflicts of interest, privacy and confidentiality and (where applicable) protection of human and animal research subjects. The authors have read and confirmed their agreement with the ICMJE authorship and conflict of interest criteria. The authors have also confirmed that this article is unique and not under consideration or published in any other publication, and that they have permission

from rights holders to reproduce any copyrighted material. Any disclosures are made in this section. The external blind peer reviewers report no conflicts of interest.

References

1. Ray A. Protease Enzyme Potential Industrial Scope. *Int J Tech.* 2012;2:1–4.
2. Gupta R, Beg QK, Lorenz P. Bacterial alkaline proteases: molecular approaches and industrial applications. *Appl Microbiol Biotechnol.* Jun 2002;59(1):15–32.
3. Stöcker W, Grams F, Baumann U, et al. The metzincins—topological and sequential relations between the astacins, adamalysins, serralsins, and matrixins (collagenases) define a superfamily of zinc-peptidases. *Protein Sci.* 1995;4:823–40.
4. Suhre K, Kristjánsson MM. Characteristics of mutants designed to incorporate a new ion pair into the structure of a cold adapted subtilisin-like serine proteinase. *Biochim Biophys Acta.* 2009;1794:512–8.
5. Gerday C, Aittaleb M, Bentahir M, et al. Cold-adapted enzymes from fundamentals to biotechnology. *Trends Biotechnol.* 2000;18:103–7.
6. Kasana RC. Proteases from psychrotrophs: An overview. *Crit Rev Microbiol.* 2010;36:134–45.
7. Wang F, Hao JH, Yang CY, Sun M. Cloning, Expression, and Identification of a Novel Extracellular Cold-Adapted Alkaline Protease, Gene of the Marine Bacterium Strain YS-80-122. *Appl Biochem Biotechnol.* 2010;162:1497–505.
8. Thomas H, Rhona EF, Robert DG, Baumann U. Crystal Structure of a Complex between *Pseudomonas aeruginosa* Alkaline Protease and Its Cognate Inhibitor. *J Biological Chem.* 2001;276:35087–92.
9. Aghajani N, Petegem FV, Villeret V, et al. Crystal structures of a psychrophilic metalloprotease reveal new insights into catalysis by cold-adapted proteases. *Proteins.* Mar 1, 2003;50(4):636–47.
10. Case DA, Darden TA, Cheatham TE III, Simmerling CL. AMBER 11. University of California, San Francisco; 2010.
11. AltschulSF, Madden TL, Schaffer AA, et al. Gapped BLAST and PSI-BLAST: a new generation of protein database search programs. *Nucleic Acids Res.* 1997;25:3389–402.
12. Gouet P, Robert X, Courcelle E. ESPript/ENDscript: extracting and rendering sequence and 3D information from atomic structures of proteins. *Nucl Acids Res.* 2003;31:3320–3.
13. Eswar N, Marti-Renom MA, Webb B, et al. Comparative Protein Structure Modeling With MODELLER. *Curr Protoc Protein Sci.* Nov 2007; Chapter 2:Unit 2.9.
14. Shen MY, Sali A. Statistical potential for assessment and prediction of protein structures. *Protein Sci.* 2006;15:2507–24.
15. Sali, A, Blundell TL. Comparative protein modelling by satisfaction of spatial restraints. *J Mol Biol.* 1993;234:779–815.
16. Eramian D, Shen MY, Devos D, et al. A composite score for predicting errors in protein structure models. *Protein Sci.* 2006;15:1653–66.
17. Laskowski RA, MacArthur MW, Moss DS, et al. PROCHECK: a program to check the stereochemical quality of protein structures. *J Appl Crystallogr.* 1993;26:283–91.
18. Colovos C, Yeates TO. Verification of protein structures: patterns of non-bonded atomic interactions. *Protein Sci.* 1993;2:1511–9.
19. Lüthy R, Bowie JU, Eisenberg D. Assessment of protein models with three-dimensional profiles. *Nature.* 1992;356:83–5.
20. Ryckaert JP, Ciccotti G, Berendsen HJC. Numerical integration of the cartesian equations of motion of a system with constraints: molecular dynamics of n-alkanes. *J Comp Phys.* 1977;23:327–41.
21. Ryckaert JP, Ciccotti G, Berendsen HJC. Numerical integration of the Cartesian equations of motion of a system with constraints: molecular dynamics of n-alkanes. *J Comput Phys.* 1997;23:327–41.
22. Wallace AC, Laskowski RA, Thornton JM. LIGPLOT: a program to generate schematic diagrams of protein-ligand interactions. *Protein Eng.* 1996;8:127–34.
23. Larkin MA, Blackshields G, Brown NP, Chenna R, McGettigan PA, Clustal W and Clustal X version 2.0. *Bioinformatics.* 2007;23:2947–8.



24. Goujon M, McWilliam H, Li W, Valentin F, Squizzato S. A new bioinformatics analysis tools framework at EMBL-EBI. *Nucleic acids research*. 2010;38 Suppl:W695–9.
25. Corpet F. Multiple sequence alignment with hierarchical clustering. *Nucl Acids Res*. 1988;16:10881–90.
26. Kabsch W, Sander C. Dictionary of protein secondary structure: pattern recognition of hydrogen-bonded and geometrical features. *Biopolymers*. 1983;22:2577–637.
27. Rost B, Sander C. Conservation and prediction of solvent accessibility in protein families. *Proteins*. 1994;20:216–26.
28. DeLano WL. *The PyMOL Molecular Graphics System*. DeLano Scientific. <http://www.pymol.org>.